Three Sources and Three Component Parts of the Concept of Dissipative Solitons

N. Akhmediev and A. Ankiewicz

Abstract We explain the notion of dissipative solitons within a historical perspective. We show that the ideas of the theory of dissipative solitons emerge from several fields, including classical soliton theory, nonlinear dynamics, with its theory of bifurcations, and Prigogine's concept of self-organization. A new notion, emerging from this three-part foundation, allows us to build the novel concept of the dissipative soliton. We also show that reductions to lower dimensional systems have to be done carefully and should always include a comparison of the results with numerical simulations of the original equations.

1 Introduction

This book is a collection of works in various fields that have the common concept of the "dissipative soliton" behind each specific topic. Before turning to the chapters, written by experts in their fields, it is instructive to start with general "definitions" and a little history of the terms. Our introductory chapter summarizes the main ideas and explains what a "dissipative soliton" entails, in simple terms. The ideas have been developed over a number of years and have appeared in various publications [1, 2, 3], but a compact presentation of all these ideas in a single volume is important.

The term "soliton" was first introduced in 1965 by Zabusky and Kruskal [4] when studying the numerical solutions of the Korteveg-de Vries equation. General solutions of this equation behaved "strangely" as a superposition of solitary waves or "solitons" and radiation waves, despite the fact that the governing equation was

N. Akhmediev
Optical Sciences Group, Research School of Physical Sciences and Engineering, Australian National University, Acton, ACT 0200, Australia, nna124@rsphysse.anu.edu.au

A. Ankiewicz
Optical Sciences Group, Research School of Physical Sciences and Engineering, Australian National University, Acton, ACT 0200, Australia

Akhmediev, N., Ankiewicz, A.: *Three Sources and Three Component Parts of the Concept of Dissipative Solitons.* Lect. Notes Phys. **751**, 1–28 (2008)
DOI 10.1007/978-3-540-78217-9_1

nonlinear. Clearly, the solitons were modes of a nonlinear system. At that point, it was understood that "waves of translation", first observed by John Scott Russell in 1834 [5], are also solitons. Later, a rigorous mathematical theory was developed [6], and this allowed us to construct a general solution of a certain class of equations in terms of solitons and radiation waves. Since this pioneering work of Gardner, Greene, Kruskal and Miura in 1967, scientists tend to use the term "soliton" to describe the modes of nonlinear partial differential equations that happen to be integrable by means of the "inverse scattering technique" [7, 8]. These "integrable" solitons do not change their shape and velocity after colliding with each other, and they remain intact when interacting with radiation waves. Occasionally, other types of localized solutions in physics were named "solitons" as well. However, this custom met serious resistance from the mathematicians who were studying "true" solitons of "integrable models".

A dramatic turning point occurred at the beginning of the 1990s, which was a time when many physicists understood the limitations of the theory. They observed the fact that "solitary waves" do exist in a variety of systems, though they do not behave exactly as the classical theory predicts for "true" solitons. In particular, "soliton-like" pulse propagation in a real optical fiber satisfies equations which are more complicated than the integrable nonlinear Schrödinger equation [9]. These equations still have solutions in the form of solitons, but they usually include additional terms that destroy integrability. The additional terms could describe physical effects, of both conservative and non-conservative nature, which modify the properties of solitons, but leave them as distinctively localized solutions of the system under consideration. Thus, the theory had to be extended, firstly, to cover localized solutions in conservative and Hamiltonian systems and later to construct a theory of solitons in systems with loss and gain. On the one hand, new solitons could not be used as superpositions in order to construct a general solution of the system, but on the other hand they appeared in physical systems as localized solutions describing certain classes of phenomena. Thus, new terms had to be used, such as "solitary pulse" for conservative systems or "dissipative soliton" in cases of systems with gain and loss. In this respect, it is worthwhile mentioning early works [10, 11] where the term "dissipative solitons" was used to describe solitons in such systems. We also have to mention that there is a very wide variety of systems with gain and loss, so that even the rather specific term "dissipative soliton" may need a finer definition in more complicated systems.

The first book "Dissipative Solitons" was published by Springer in 2005 [12]. This was the time when major principles had to be unified and presented in a single volume. This first attempt turned out to be highly successful. It generated a multiplicity of ideas and brought the scientific community to the idea of organizing a workshop with the same name. The workshop took place in January 2006 in Dresden, Germany, within the Max Planck Institute for Physics of Complex Systems. This meeting solidified the ideas behind the concept of "dissipative solitons". It also became clearer than ever that the notion of "dissipative solitons" could be applied to biology and even medicine, and hence not only to physical systems. Hence, in publishing this book, the editors attempt to spread these ideas broadly and attract

more scientists to consider localized solutions from the new point of view. This may open new facets in the perception of known phenomena, as well as assisting in the understanding of novel phenomena.

The dissipative soliton concept is a fundamental extension of that for solitons in conservative and integrable systems. It includes ideas from three major sources, viz. standard soliton theory developed since the 1960s, ideas from nonlinear dynamics theory and Prigogine's ideas of systems far from equilibrium and self-organization (see Fig. 1). These are basically the three sources and three component parts of this novel paradigm. Physically speaking, the major part of standard soliton theory is the notion of the balance between dispersion and nonlinearity that allows stationary localized solutions to exist. For dissipative systems, we need to observe that the important balance is between gain and loss – this condition is necessary for solitons to be stationary objects. Even the slightest imbalance will result in the solution either growing indefinitely, if gain prevails, or disappearing completely because of the dissipation. Thus, instead of a single balance, we have to consider a composite balance between several physical phenomena.

The second part of our foundation – nonlinear dynamics – inspires us with the idea of a soliton as a fixed point of an infinite-dimensional dynamical system. Stability properties of fixed points determine the stability of the soliton itself. Fixed points can be transformed into limit cycles at certain values of the system parameters, and then the soliton becomes a pulsating object. Further transformations may include irregular behavior of the trajectory, thus creating chaotic solitons. Therefore, nonlinear dynamics supplies us with the ideas of soliton bifurcations and the chaotic

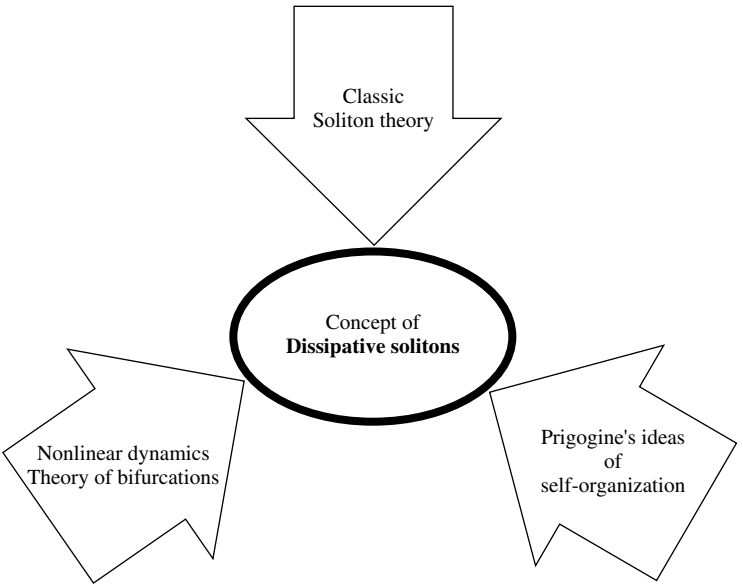

Fig. 1 Three sources and three component parts of the concept of dissipative solitons

evolution of solitons. Since we consider infinite-dimensional dynamical systems, there is a huge variety of types of solitons and their bifurcations.

Finally, the third part of the basis – the theory of systems far from equilibrium – tells us that solitons are self-organized formations requiring a continuous supply of matter or energy. As soon as that supply finishes, a dissipative soliton ceases to exist. In simple terms, self-organization is a convergence of certain initial conditions to a localized solution of the system that is stable for a given set of external parameters. Thus, the final state is determined by the physical laws and not by the initial condition. For infinite-dimensional dynamical systems, this stable solution can be very complicated. It is not necessarily a smooth function with a single maximum and exponentially decaying tails. Moreover, there can be several stable solutions existing for the same set of parameters. This can even happen in the case of a relatively simple equation like the complex cubic-quintic Ginzburg–Landau equation. The majority of processes in nature are governed by far more complicated dynamical factors. Thus, stationary solutions of these systems can be considerably more involved.

From this point of view, the idea of self-organization allows us to extend the concept of dissipative solitons to highly complicated objects such as animal species and the formation of life itself. How far we can go in extending our principles in this direction only depends upon our imagination. Adding to this complexity, when a system converges to a solution, is not necessarily a stationary solution but can be a limit cycle or a strange attractor in an infinite-dimensional phase space. Many biological processes such as heart beats and nerve pulse propagation have been described using simple mathematical modeling. Scientific progress in this direction continues and the reader can find some examples in other chapters of this book.

There is the older term "autosoliton" which comes from the book by Kerner and Osipov [13]. As the title of the book suggests, the authors consider localized solutions from Prigogine's point of view as self-organized structures. As we can see from Fig. 1, this is one of the foundation stones of the new concept. More specifically, the name "autosoliton" came naturally from the theory of reaction-diffusion systems [14]. Usually, it had to be supplemented with the notions of "activator" and "inhibitor" to be understood in its full complexity. The root of the word itself originates from the term "auto-oscillations" in the theory of "flutter and shimmy" which can be understood as "self-propelled" solitons. In a few cases, this term has even been used in optics. Throughout this book, the term "dissipative soliton" is used as the one that covers the majority of relevant phenomena in optics, biology and medicine. As a fuller explanation, it means "soliton in a dissipative system", where "dissipative system" is to be understood in Prigogine's sense as a sub-system with an external pump of energy, rather than a system with losses only. An optical laser is one of the examples of such subsystem in optics [15].

There is a significant difference between solitons in Hamiltonian systems and in dissipative ones. In Hamiltonian systems, soliton solutions appear as a result of a balance between diffraction (or dispersion) and nonlinearity. Diffraction spreads the beam, while nonlinearity focuses it and makes it narrower. The balance between the two results in stationary solutions. These usually form a one-parameter family. In

systems with gain and loss, in order to have stationary solutions, gain and loss must be balanced in the first place. The two balances result in solutions which are fixed. The shape, amplitude and the width are all fixed and depend on the parameters of the equation. This situation is represented qualitatively in Fig. 2. For telecommunication applications, the rigidity of the soliton may provide efficient suppression of noise and stop any drift in the soliton parameters.

Clearly, stationary dissipative solitons can be considered as fixed points of an infinite-dimensional dynamical system. Thus, their parameters are fixed. These formations are stable on propagation, provided the system parameters are chosen in appropriate regions. In general, dissipative solitons are not necessarily stationary. In other words, fixed points are not the only objects that may exist in such systems. For example, a limit cycle is another, more complicated, object that can exist in the phase space of the dynamical system. It corresponds to a pulsating soliton where the parameters oscillate periodically [25]. These solitons usually exist in regions of the parameter space which are adjacent to those of stationary solitons. However, even in this case, the soliton characteristics are fixed, i.e., the period of the pulsations and the shapes at particular points of the period are all fixed, since they are functions

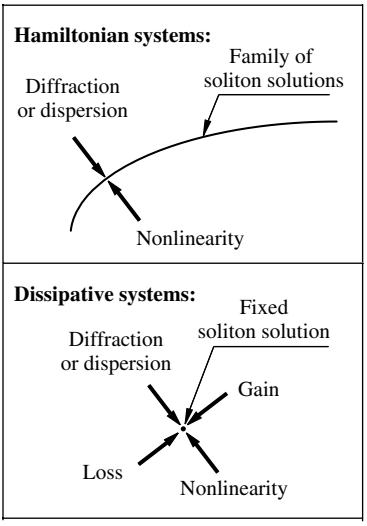

Fig. 2 Qualitative difference between soliton solutions in Hamiltonian and dissipative systems [1]. In Hamiltonian systems, soliton solutions are the result of a single balance, and comprise one- or few-parameter families, whereas, in dissipative systems, the soliton solutions are the result of a double balance and, in general, are isolated. There can be exceptions to this rule [16, 17, 18], but, usually, the solutions are fixed (i.e., isolated from each other). On the other hand, it is quite possible for several isolated soliton solutions to exist for the same equation parameters. This is valid for (1+1), (2+1) dimensional as well as for (3+1) dimensional cases. In the latter case, the terms "localized structures" [19] and "bullets" [20, 21, 22, 23] are also used, along with the term "solitons" [24]

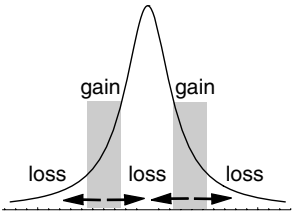

Fig. 3 Qualitative description of solitons in dissipative systems [1]. The soliton has areas of consumption as well as expenditure of energy, and these can be both frequency (spatial or temporal) and intensity dependent. *Arrows* show the energy flow across the soliton. The soliton is the result of complicated dynamical processes of energy exchange with the environment and between its own parts

of the system parameters. One more possibility is that the dissipative soliton can be chaotic [25]. If the soliton is chaotic, the characteristics of this chaotic behavior are also given by the parameters of the system.

Another simple qualitative picture is presented in Fig. 3. In order to be stationary, solitons in dissipative systems need to have regions where they extract energy from an external source, as well as regions where energy is dissipated to the environment. A stationary soliton is the result of a dynamical process of continuous energy exchange with the environment and its redistribution between various parts of the soliton. As soon as this energy redistribution ends, the soliton disappears. In more complicated cases, a matter exchange is involved as well. In this sense, the dissipative soliton is more like a living thing than an object of the inanimate world. It is like a species in biology which is fixed (or isolated) in its properties.

So we have just described, albeit briefly, the basic cornerstones of the powerful concept of the dissipative soliton, and we present them schematically in Figs. 1, 2 and 3. Our observations are mostly related to dynamical systems whose evolution can be described by differential equations with partial derivatives. Such dynamical systems have an infinite number of degrees of freedom and, surely, they may have a countless number of soliton solutions with a countless number of bifurcations between them. As a rule, these systems are non-integrable, which means that exact solutions in their full complexity can be studied only numerically. To describe fine features of soliton bifurcations analytically, we need approximations and some techniques to reduce the dimensionality of the dynamical system. These methods may help, to some extent, in describing stationary or pulsating solitons and their bifurcations over a limited range of the system parameters. However, they cannot be used as a total substitute for rigorous studies of the solutions. Only the most prominent features of the solitons, along with selected bifurcations, can be determined in this way. For a full picture, we still need numerical simulations. In the rest of this chapter, we give a few examples of studies that involve reductions to finite-dimensional approximations. We also show that direct comparisons with the results of numerical simulations are essential in these studies.

2 Cubic-Quintic Complex Ginzburg–Landau Equation

Throughout this chapter, we are dealing with an infinite-dimensional dynamical system governed by the cubic-quintic complex Ginzburg–Landau equation (CGLE) which in optics has been widely used to describe the pulsed operation of passively mode-locked lasers and all-optical long-haul soliton transmission lines. Generally, the CGLE has a wide range of applications in various branches of physics, chemistry and biology. An extensive list of applications can be found in the review paper by Aranson and Kramer [26]. This enormous sphere of knowledge has been dubbed "The world of the Ginzburg–Landau equation" [26]. The cubic-quintic complex equation has so many different types of solutions that this area of expertise is a whole world by itself. Even if we restrict ourselves to localized solutions, i.e., dissipative solitons of CGLE, the variety of these objects is still not known in its full complexity although the regions of soliton existence have been studied quite extensively [27, 28, 29].

One of the difficulties is that analytic solutions are known only for a special class of CGLE solitons [30] when parameters of the equation are related by a specific algebraic equation. All other soliton solutions can only be found numerically. One of the features of these solutions is that they have rich structure of bifurcations [31, 32]. Having this structure leaves little hope for exact analytical description. Nevertheless, approximate methods are always a possibility. Such approximations are the main subject in the rest of this chapter. We give an example of the application of the so-called method of moments, which allows us to approximate, for example, periodicity in the motion of the soliton and the bifurcation from stationary to pulsating solitons. We stress that only simple properties of the dissipative solitons can be approximated by employing reductions. Using this technique, we consider three examples where simple approximations can give qualitative descriptions of the soliton behavior and even predict the existence of unknown branches of solitons.

In our notation, the CGLE is

$$\mathrm{i}\psi_t + \frac{D}{2}\,\psi_{xx} + |\psi|^2\psi + \nu|\psi|^4\psi = \mathrm{i}\delta\psi + \mathrm{i}\varepsilon|\psi|^2\psi + \mathrm{i}\beta\psi_{xx} + \mathrm{i}\mu|\psi|^4\psi. \qquad (1)$$

When used to describe passively mode-locked lasers, the CGLE represents a distributed propagation model, in which t is the distance traveled inside the cavity, x is the retarded time, ψ is the normalized envelope of the field, D is the group velocity dispersion coefficient, with $D = \pm 1$, depending on whether the group velocity dispersion (GVD) is anomalous or normal, respectively, δ is the linear gain–loss coefficient, $\mathrm{i}\beta\psi_{xx}$ accounts for spectral filtering or linear parabolic gain ($\beta > 0$), $\varepsilon|\psi|^2\psi$ represents the nonlinear gain (which arises, for example, from saturable absorption), the term with μ represents, if negative, the saturation of the nonlinear gain, while the one with ν corresponds, also if negative, to the saturation of the nonlinear refractive index.

During numerical computations with the propagation equation, the magnitude that we most often monitor is the energy, Q, carried by a certain solution after a propagation distance of t. It is defined by

$$Q = \int_{-\infty}^{\infty} |\psi(x,t)|^2 \mathrm{d}x.$$

For a dissipative system, Q is a function of t rather than a conserved quantity. The convenience of monitoring the energy Q is clear from the following considerations. For localized solutions, Q is finite. Decaying solutions result in Q converging to zero. When the localized solution is stationary, Q takes a constant value. Stable localized solutions show convergence of Q to a constant when starting from an initial condition that is not a solution of the CGLE. Thus, stability of a soliton obtained this way follows directly from numerical simulations. When the soliton solution is pulsating in t, the quantity Q also oscillates on propagation. In this instance, we denote its maxima and minima of Q by Q_{M} and Q_{m}, respectively. Chaotic solitons generally produce chaotic evolution of Q. Of course, a more detailed study of solitons should involve more of these integral parameters. However, there will always be a limitation because of the gap between the finite number of the parameters that we are able to use and the fact that our dynamical system has an infinite number of degrees of freedom.

3 The Method of Moments

In this section, we briefly outline the approach that we use to derive the dynamical model. The method of moments [33] is a reduction of the complete evolution problem with an infinite number degrees of freedom to the evolution of a finite set of pulse characteristics. For a localized solution with a single maximum, these characteristics include the peak amplitude, pulse width, center-of-mass position and phase parameters. For an arbitrary localized field, one can introduce two integrals, namely the energy Q and momentum M,

$$Q = \int_{-\infty}^{\infty} |\psi|^2 \mathrm{d}x, \quad M = \frac{1}{2} \int_{-\infty}^{\infty} (\psi \psi_x^* - \psi^* \psi_x) \mathrm{d}x, \tag{2}$$

and higher-order generalized moments [33],

$$I_1 = \int_{-\infty}^{\infty} x|\psi|^2 \mathrm{d}x, \quad I_2 = \int_{-\infty}^{\infty} (x-x_0)^2 |\psi|^2 \mathrm{d}x,$$

$$I_3 = \int_{-\infty}^{\infty} (x-x_0)(\psi^* \psi_x - \psi \psi_x^*) \mathrm{d}x. \tag{3}$$

The number of higher-order generalized moments is infinite. Depending on the complexity of the reduced model, we can restrict ourselves to a finite number of them. Using the original equation (1), we can derive the evolution equations for the generalized moments [33],

$$
\begin{aligned}
\frac{\mathrm{d}Q}{\mathrm{d}t} &= \mathrm{i}\int_{-\infty}^{\infty}(\psi R^* - \psi^* R)\mathrm{d}x,\\
\frac{\mathrm{d}M}{\mathrm{d}t} &= -\mathrm{i}\int_{-\infty}^{\infty}(\psi_x R^* + \psi_x^* R)\mathrm{d}x,\\
\frac{\mathrm{d}I_1}{\mathrm{d}t} &= \mathrm{i}DP + \mathrm{i}\int_{-\infty}^{\infty} x(\psi R^* - \psi^* R)\mathrm{d}x,\\
\frac{\mathrm{d}I_2}{\mathrm{d}t} &= -\mathrm{i}DI_3 + \mathrm{i}\int_{-\infty}^{\infty}(x-x_0)^2(\psi R^* - \psi^* R)\mathrm{d}x,\\
\frac{\mathrm{d}I_3}{\mathrm{d}t} &= 2P\frac{\mathrm{d}x_0}{\mathrm{d}t} + \mathrm{i}\int_{-\infty}^{\infty}(2D|\psi_x|^2 - |\psi|^4)\mathrm{d}x\\
&\quad + 2\mathrm{i}\int_{-\infty}^{\infty}(x-x_0)(\psi_x R^* + \psi_x^* R)\mathrm{d}x\\
&\quad + \mathrm{i}\int_{-\infty}^{\infty}(\psi R^* + \psi^* R)\mathrm{d}x.
\end{aligned}
\tag{4}
$$

Equations (4) are quite general, i.e., they are valid for a large class of NLSE-type evolution equations, including (1) with arbitrary coefficients. Up to this point, the equations are exact if we use an exact solution of (1) for ψ.

In practice, one uses a trial function with a few parameters which depend on t. Equations for the evolution of these parameters are found from a system similar to (4). A suitable choice of trial function can be deduced from the general symmetries of the problem, and from results of experiments and numerical simulations. The minimum number of parameters needed to describe localized solutions is usually five (see Sect. 4). More parameters may improve the accuracy, but the complexity of the analysis then increases dramatically. Since the number of the moments should correspond to the number of the parameters, we consider only five moments.

The method of moments has been applied to various problems described by the perturbed NLSE [33, 34, 35]. The method was also used for the CGLE in [36, 37, 38], where simplified trial functions were considered. For special problems, even the first two equations (4) may be sufficient when we deal with specific two-dimensional reductions of the CGLE [39]. In more complicated cases, we need more equations. It turns out that the complete set of equations (4) is the minimum required for modeling the pulsating solitons.

4 Pulsating Solitons and Their Approximations [37, 38]

A pulsating soliton is a localized solution of the CGLE that changes its width, amplitude and other parameters periodically in t. A pulsating soliton is a limit cycle of the infinite-dimensional dynamical system and can be described by a closed loop in the phase space of the system. Exact analytical solutions for pulsating solitons are not known. Thus, we have to use finite-dimensional approximations. One of them is an approximation using a trial function with a finite number of variable parameters. The choice of trial function is usually motivated by numerical simulations of the CGLE (1). It was found [25, 31, 40] that for various sets of the system parameters, a dissipative soliton is a single-humped pulse with phase modulation. We consider two forms of the trial function in order to demonstrate that the results may vary, but qualitative features of the solution can be picked up, provided a reasonable choice of the function has been made.

4.1 Trial Function: Sech-Pulse

The first type of trial function that we use has the form of a *sech*-function:

$$\psi(x,t) = A\ \mathrm{sech}\left(\frac{x-x_0}{w}\right)\exp\left[\mathrm{i}\left[\phi + b(x-x_0) + c(x-x_0)^2\right]\right], \tag{5}$$

where $A(t)$, $w(t)$ and $x_0(t)$ are the amplitude, width and position of the pulse maximum, respectively, $\phi(t)$ is the phase shift, $b(t)$ is the linear phase coefficient, and $c(t)$ is the chirp parameter. The phase in (5) is expanded up to the second order. This form differs from the trial function used in [36], where only linear terms in the phase were considered. We emphasize that the chirp is highly important for solutions of the CGLE. As numerical simulations show, even stationary solitons have appreciable phase modulation, not to mention more complicated localized waves, such as pulsating and exploding solitons.

Now, the generalized moments can be expressed in terms of the soliton parameters in the trial function. Evaluation of integrals (2) and (3), with the help of (5), gives the following expressions:

$$\begin{aligned} &Q = 2A^2 w, \quad M = -2\mathrm{i}A^2 wb, \quad I_1 = 2A^2 wx_0, \\ &I_2 = (\pi^2/6)A^2 w^3, \quad I_3 = \mathrm{i}(2\pi^2/3)A^2 w^3 c. \end{aligned} \tag{6}$$

Then, using (4), one can obtain a set of ordinary differential equations for the soliton parameters in (5):

$$Q_t = F_1 \equiv 2Q\left[\delta - \beta\left(b^2 + \frac{1}{3w^2} + \frac{\pi^2}{3}c^2w^2\right) + \frac{\varepsilon}{3}\frac{Q}{w} + \frac{2\mu}{15}\frac{Q^2}{w^2}\right],$$

$$w_t = F_2 \equiv 2Dcw + \beta\left(\frac{8}{\pi^2 w} - \frac{16\pi^2}{15}c^2 w^3\right) - \frac{2\varepsilon}{\pi^2}Q - \frac{\mu}{\pi^2}\frac{Q^2}{w},$$

$$c_t = F_3 \equiv 2D\left(\frac{1}{\pi^2 w^4} - c^2\right) - \frac{1}{\pi^2}\frac{Q}{w^3} - 4\left(\frac{1}{3} + \frac{1}{\pi^2}\right)\beta\frac{c}{w^2} - \frac{8\nu}{15\pi^2}\frac{Q^2}{w^4}. \quad (7)$$

We have made additional reductions in (7), namely two equations

$$x_{0,t} = F_4 \equiv b\,(D - \frac{2\pi^2}{3}\beta c w^2),$$

$$b_t = F_5 \equiv -\frac{4}{3}\beta\,(\frac{1}{w^2} + \pi^2 c^2 w^2)\,b, \quad (8)$$

can be removed. For $\beta > 0$, the value of the linear phase b tends to zero for $t \to \infty$. Then, the soliton center $x_0(t)$ tends to a *constant* value for $t \to \infty$. This allows us to consider a system with only three variables, viz. Q, w and c. In other words, the three-dimensional subset describes the asymptotic dynamics of the five-dimensional model (7) for $t \to \infty$.

4.2 Trial Function: Generalized Gaussian Pulse

As numerical simulations show [25, 31], pulsating solitons change their shape during one period from a bell-shaped pulse to a flat-top pulse. Therefore, we consider a second trial function which is a combination of Gaussian and super-Gaussian types of functions:

$$\psi(x,t) = A\exp\left(-\frac{x^2}{w^2} - \frac{x^4}{4m w^4} + \mathrm{i}\,c x^2\right), \quad (9)$$

where $A(t), w(t)$ and $c(t)$ have the same meaning as in (5). The constant m can be chosen arbitrarily, but it is independent of t. Note that, following the discussion in Sect. 4.1, $x_0(t)$ and the linear phase b are taken to be zero implicitly in the ansatz. This leaves three parameters, A, w and c, to be found from the three-dimensional model.

The trial function (9), with $m > 0$, gives better results than the *sech* function or the Gaussian function alone or the super-Gaussian function with a quartic term alone. Also, the case $4m = 1$ agrees well with the numerical simulations of the CGLE. However, this value is not critical and other values of m can be used.

Since the function (9) is symmetric in x, the integrals M and I_1 are identically zero. Other moments in (2) and (3), for $4m = 1$, are given by

$$Q = 1.051A^2 w, \quad I_2 = 0.1448Qw^2, \quad I_3 = \frac{\mathrm{i}}{4}\,c I_2. \quad (10)$$

Then (4) results in the following dynamical model ($4m = 1$):

$$Q_t = F_1 \equiv \frac{Q}{w^2}\left[2\delta w^2 - 3.737\beta - 1.158\beta c^2 w^4 + 1.433\varepsilon w Q + 1.143\mu Q^2\right],$$

$$w_t = F_2 \equiv \frac{1}{w}\left[2.142\beta + 2cw^2 - 0.8738\beta c^2 w^4 - 0.2896\varepsilon w Q - 0.3254\mu Q^2\right],$$

$$c_t = F_3 \equiv \frac{1}{w^4}\left[6.453 - 2c^2 w^4 - 1.237 w Q - 1.319\nu Q^2 - 19.62\beta w^2 c\right]. \quad (11)$$

As expected, the equations for Q_t, w_t and c_t in (7) and (11) are similar. The only difference lies in the numerical values of the coefficients of the terms.

4.3 Fixed Points and Their Stability [38]

Fixed points (FPs) of (7) with $x_0 = b = 0$, or of (11), are found from the set of algebraic equations $F_j = 0,\ j = 1,2,3$. The stability of the FPs is determined from the analysis of the eigenvalues λ_j, $j = 1,2,3$, of the Jacobian matrix $M_{ij} = \partial F_i/\partial p_j$, where $\{p_1, p_2, p_3\} \equiv \{Q, w, c\}$, and $i = 1,2,3$. When the real part of any eigenvalue becomes positive, the corresponding fixed point becomes unstable. Since the characteristic equation for the eigenvalues is cubic, either $\lambda_1 = \lambda_2^*$ and λ_3 is real or all three λ_j are real.

We analyze the models (7) with $x_0 = b = 0$ and (11) for different signs of D and values of the parameters ν, ε, μ and β. We set $\delta = -0.1$. Firstly, we compare the results of numerical simulations of the CGLE (1) with those of the models (7) and (11). The results of numerical simulations of the CGLE (1) for $\beta = 0.08$ and $\mu = -0.1$ are shown in Fig. 4a. The figure shows the bifurcation boundaries between various types of localized waves that exist at particular values of the system parameters. The region with vertical shading corresponds to stationary solitons. Solutions describing two fronts moving in opposite directions exist in the region with horizontal shading. Pulsating solitons with periodic or chaotic variations of their parameters occupy the area between these two regions.

There are four types of fixed points for the three-dimensional model:

$$\begin{aligned} S_1 &= \{(-,+),\ \lambda_1^\star,\ (-,0)\},\\ S_2 &= \{(-,0),\ (-,0),\ (-,0)\},\\ U_1 &= \{(+,+),\ \lambda_1^\star,\ (-,0)\},\\ U_2 &= \{(-,+),\ \lambda_1^\star,\ (+,0)\}, \end{aligned} \quad (12)$$

where the variables in curled brackets are complex eigenvalues $\{\lambda_1, \lambda_2, \lambda_3\}$ of the fixed point. The symbols in parentheses show that the corresponding parts of $\lambda_j = (\mathrm{Re}\lambda_j, \mathrm{Im}\lambda_j)$ are either positive (+), negative (−) or zero. The types S_1 and S_2 (U_1 and U_2) correspond to stable (unstable) FPs.

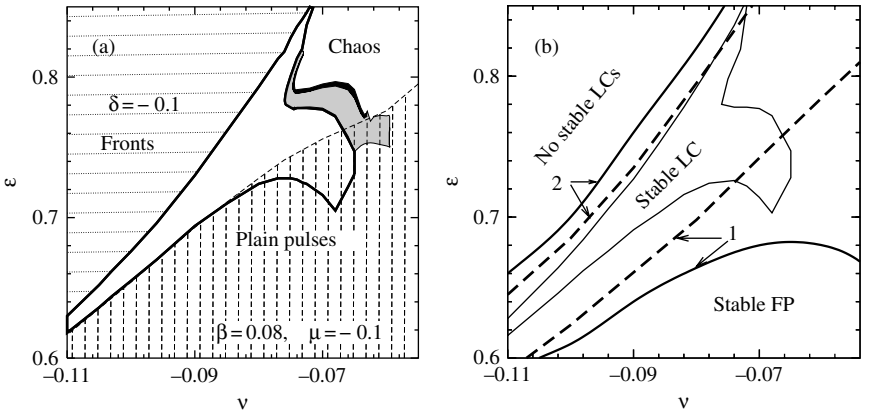

Fig. 4 (**a**) Regions of existence of various solutions obtained from numerical simulations [31] of the CGLE (1). (**b**) Regions of existence and stability of FPs and limit cycles of the reduced systems in (ν, ε)-plane. The region between the two *solid* [*dashed*] *lines*, 1 and 2, corresponds to the region of existence of stable LCs in the models Eqs. (7) [Eqs. (11)]. The region for pulsating solitons is copied from (**a**) to (**b**) for comparison. The system parameters are shown in (**a**)

The bifurcation diagram for the models (7) and (11) is shown in Fig. 4b. When the value of gain, ε, is small, there are no FPs in the system. The threshold for FP existence, ε_{ex}, can be estimated roughly as $\varepsilon_{\text{ex}} \approx 2\sqrt{\delta\mu}$. For the parameters in Fig. 4, $\varepsilon_{\text{ex}} \approx 0.2$. If $\varepsilon > \varepsilon_{\text{ex}}$, then there are two FPs. In the region below the solid [dashed] curve 1 for model (7) [for model (11)], one FP is of the type S_1, while the other FP is of the type U_2. The second point, U_2, does not change its type and is unstable in the whole square region shown in Fig. 4b. Therefore, the bifurcation line 1 in Fig. 4b is related to the transformation of the first FP.

Curve 1 is the bifurcation boundary (threshold) where the stable FP of type S_1 becomes an unstable one of type U_1. The following condition is satisfied at the threshold:

$$\text{Re}[\lambda_1] = \text{Re}[\lambda_2] = 0. \tag{13}$$

The loss of stability of an FP can either be a result of merging with another unstable FP or be due to the creation of (annihilation with) a *limit cycle* [41]. The latter transition corresponds to a super-critical (sub-critical) Hopf bifurcation [41]. Since the number of the FPs does not change in the whole area in Fig. 4b, the curve 1 is related to the threshold of the Hopf bifurcation in the models (7) and (11).

If the Hopf bifurcation is super-critical, a stable LC would appear exactly at the same value of ε where the FP loses stability. When the Hopf bifurcation is sub-critical, the stable LC should appear before the FP becomes unstable [41]. In the latter case, the stable FP and stable LC co-exist for a certain interval of the system parameters. Numerical simulations of (7) and (11) show that for the set of parameters in Fig. 4b, the bifurcation is super-critical. The loss of stability of the FP S_1 is accompanied by the creation of a *stable* limit cycle (LC).

Close to curve 2 in Fig. 4b, the period of the LC tends to infinity. There is no stable LC above curve 2. The soliton energy Q and width w in this region increase monotonically with t, while the ratio Q/w, which is related to the square of the soliton amplitude A^2 [see (6) and (10)], remains roughly constant.

The region in Fig. 4b surrounded by the thin solid curve corresponds to the area of existence of pulsating solitons of CGLE, as found from direct numerical simulations. It is copied from Fig. 4a. A comparison of Fig. 4a and b shows a clear correspondence between the attractors (FPs and LCs) of the two models (7) or (11) and stable localized solutions of the CGLE. Specifically, an FP of the model (7) or (11) corresponds to a stationary soliton, and an LC obtained in the reduced model corresponds to a pulsating soliton. The solution with almost constant A and increasing w (the area above the curve 2 in Fig. 4b) approximates two fronts moving in opposite directions. Such a solution was observed in numerical simulations of the CGLE [31]. The boundaries obtained in each of the reduced models are fairly close to the exact ones. Thus, each of the models (7) and (11) provides a reasonably good qualitative description of soliton bifurcations inside the squared area of Fig. 4.

In contrast to the stationary state, LCs or pulsating solitons appear due to the *dynamic* balance between dissipation and energy supply. Pulsations involve periodic variations of the soliton-shape parameters A and w and the phase parameter c. This behavior is similar to transient dynamics in the integrable NLSE [42], when a non-soliton pulse adjusts its form to the fundamental soliton via quasi-periodic changes of its amplitude and phase. In the case of the NLSE, such oscillations are damped because the pulse loses energy, radiating linear waves during the transient stage. In the case of pulsating solitons of the CGLE, such oscillations are undamped due to the continuous energy supply.

The parameters of the LC change between curves 1 and 2. The oscillation period of the LC is finite on curve 1 but it varies along this curve. It is inversely proportional to $\mathrm{Im}[\lambda_1]$ of the first FP. The period increases monotonically with ε at any fixed ν. As mentioned above, the oscillation period of the LC becomes infinite on curve 2, and the LC disappears above it. Examples of limit cycles in three-dimensional phase space for two different sets of parameters are presented in Fig. 5.

The dependence of the oscillation period of the LCs on ε, when other parameters are fixed, is shown in Fig. 6 for each of the reduced models. The curve (solid line), obtained from direct numerical simulations of the CGLE (1), is also shown for comparison. There is an apparent difference in the numerical values of the period due to the drastic reduction in the number of degrees of freedom in the models. However, all three curves have the same qualitative behavior. In particular, each curve starts with a finite value of the period T at the lower boundary of the region where pulsating solitons exist. The period T increases to infinity when ε reaches the upper boundary. It is clear that the function given by (9) gives more accurate results.

A comparison of the actual field evolution in z with the one reconstructed from the reduced model is presented in Fig. 7. The results of numerical simulations of the CGLE (1) are shown in Fig. 7a. The field reconstructed from the ansatz (5) and the dynamical systems (7) is plotted in 7b. The qualitative features of the dynamics are

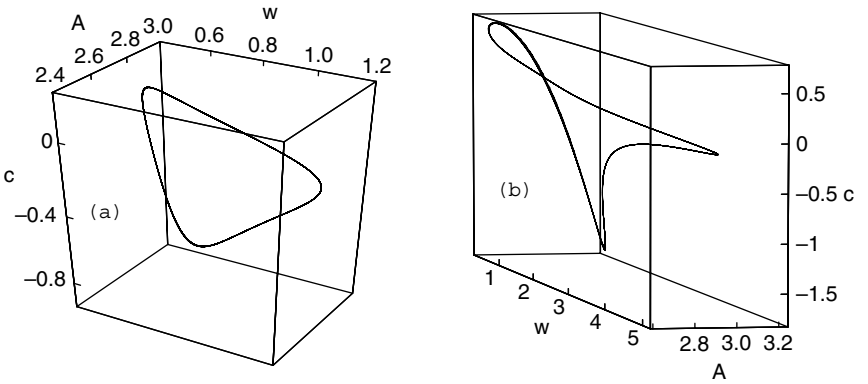

Fig. 5 Examples of limit cycles in (A, w, c)-space for the model (7), $\beta = 0.08$, $\mu = -0.1$ and $\nu = -0.09$. (**a**) $\varepsilon = 0.66$. (**b**) $\varepsilon = 0.72$

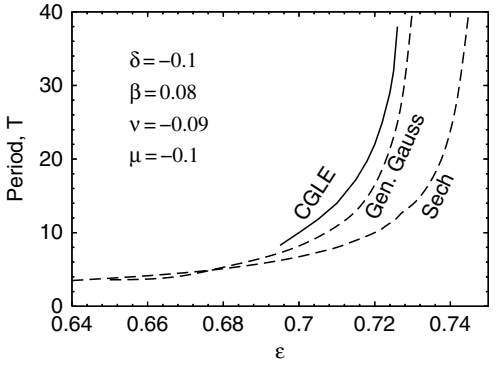

Fig. 6 Period of pulsations, T, as function of ε. The *solid line* is the result of numerical simulations of the CGLE (1). The *dashed lines* correspond to the models (7) and (11)

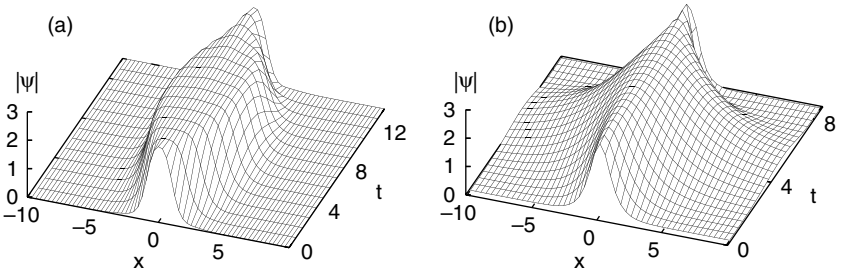

Fig. 7 (**a**) Pulsating soliton found from numerical simulations [31] of (1). (**b**) Soliton reconstructed from the trial function (5) and solution of (7). The system parameters are $\beta = 0.08$, $\varepsilon = 0.66$, $\mu = -0.1$ and $\nu = -0.1$

similar. In particular, the soliton width varies periodically, while the soliton amplitude is close to a constant in each case.

The limited range of parameters in Fig. 1b is chosen in order to establish a correspondence with the known numerical results for CGLE. A comparison of the results obtained from (7) and (11) with the numerical simulations of the full CGLE justifies the validity of the models. Therefore, one can expect that the dynamical systems (7) and (11) will be useful for predicting the bifurcation thresholds in a wider range of the system parameters [38].

5 Creeping Solitons [32, 43]

A creeping soliton is a special type of pulsating localized solution that changes its shape periodically and shifts a finite distance in the transverse direction after each period of oscillation. The value of the shift is constant for each period so that the soliton has a finite average velocity, although the motion occurs as a step-by-step translation in one direction. In most cases, solitons that move in this way have long flat-top profiles that consist of two fronts at the sides of the soliton. The two fronts move asymmetrically in time, thus creating creeping movements of the whole "worm-like" formation. An example is given in Fig. 8.

Creeping solitons were first observed in numerical simulations in [44]. Their existence for various dissipative systems has been confirmed in later publications [31, 45]. There is no technique that would allow us to describe pulsating solutions using exact solutions of the governing equation. Consequently, we have little hope of finding analytical solutions for creeping solitons. The method of moments allows us to approximate roughly the creeping motion. As a particular result, it allows us not only to estimate the period of the pulsations but to include in the model the possibility of translational motion of localized solutions. This requires an additional variable for the velocity of the soliton, and this increases the dimensionality of the finite-dimensional dynamical system. The velocity is also a periodic function of time, and it thus describes the creeping feature of the soliton. The technique also

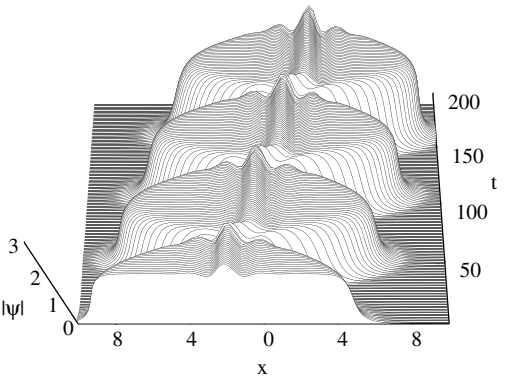

Fig. 8 An example of a creeping soliton of the CGLE. This numerical example was first found in [31]. The present simulation shows more detailed structure of creeping behavior. The asymmetric motion of the two sides of the soliton is clearly visible. The parameters of the equation are $D = 1$, $\delta = -0.1$, $\beta = 0.101$, $\varepsilon = 1.3$, $\mu = -0.3$ and $\nu = -0.101$

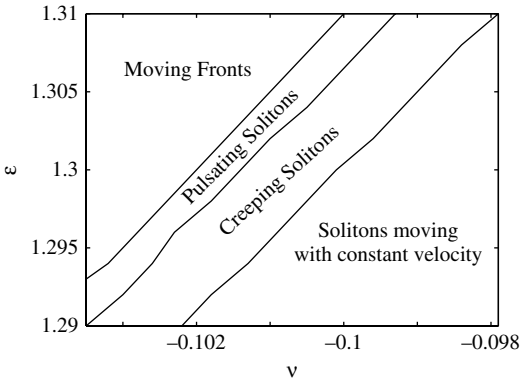

Fig. 9 Region of existence of creeping solitons found by solving the CGLE with δ, β and μ fixed at -0.1, 0.101 and -0.3, respectively. Creeping solitons exist in the central diagonal strip of this plot. Above it, there is a strip that corresponds to pulsating solitons with zero velocity. Above the upper line, solitons increase their width indefinitely, thus transforming into a pair of fronts. Below the central diagonal strip, solitons have stationary profiles and move with constant velocities

allows us to estimate the region of existence of creeping solitons in the space of equation parameters.

Creeping solitons exist in a certain range of the equation parameters. Previously, only isolated examples had been found [31]. Finding the complete region requires extensive numerical simulations. The results of simulations are summarized in Fig. 9. Creeping solitons exist in the central diagonal strip of the (ε, ν) plane. Below this strip, pulsations disappear and pulses are transformed into fixed shape solitons moving with constant velocity. These constant profile pulses are moving along the x-axis. Above the diagonal strip, the pulses are still pulsating but their average velocity is zero. Thus, the creeping feature disappears at the middle solid curve in Fig. 9. Inside the strip, the soliton energy oscillates due to the oscillations of the soliton width. These oscillations are shown in Fig. 10a. The period of the oscillations varies in the range 50–60 across the strip. In each oscillation, the center of mass of the soliton moves by a finite increment. This step wise motion of the center of mass is shown in Fig. 10b. Due to the symmetry of the CGLE with respect to the inversion of the x-axis, a soliton can equally well move to the left or to the right, depending on the initial condition.

5.1 The Choice of Trial Function for Creeping Solitons

As numerical simulations show, a creeping soliton changes its shape during one period from a bell-shaped pulse to a flat-top pulse. Its velocity is generally a constant with an irregular ripple superimposed on it. Therefore, we consider a trial function which is a generalization of a "super-Gaussian" function:

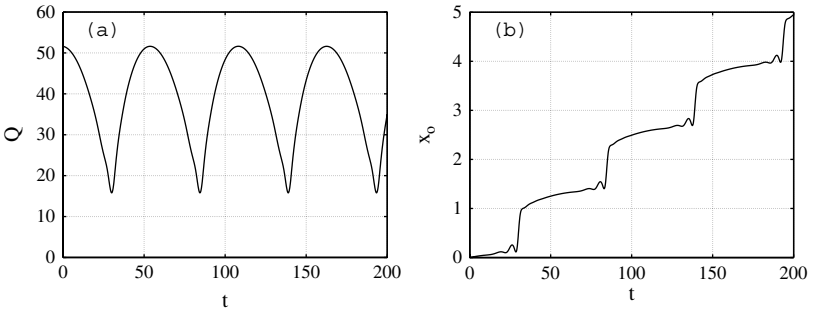

Fig. 10 (**a**) Soliton energy Q vs t for a creeping soliton at the point $\varepsilon = 1.3$, $\nu = -0.101$. The energy oscillates in a wide range showing that the width of the soliton changes appreciably. (**b**) Center of mass of the same soliton vs t. The soliton moves step by step in the direction of increasing x. Due to the symmetry in x, the soliton could also move in the opposite direction if the initial condition was changed

$$\psi(x,t) = a(m)\sqrt{\frac{Q(t)}{w(t)}}\exp\left[-\frac{\sqrt{m}\,y}{w(t)} - \frac{y^4}{32\,w^4(t)} + \mathrm{i}\left(b(t)\,y + c(t)\,y^2\right)\right], \qquad (14)$$

where $y = x - x_0(t)$, $w(t)$ is the width, $b(t)$ and $c(t)$ are the linear part and the quadratic part of the chirp, respectively. The constant m can be chosen arbitrarily, but it is independent of t, while a is a constant that depends on m. It is chosen in such a way that the total energy, $\int_{-\infty}^{\infty} |\psi|^2\,\mathrm{d}x$, equals $Q(t)$. For example, if $m = 0.008$, we have $a = 0.519548$. The trial function given in (14) is deliberately chosen to be non-symmetric in y, otherwise the velocity and linear chirp will approach zero after a short transient. This would mean that we would then effectively have only three ODEs, and the creeping effect could be lost. Using the above trial function, we are still able to obtain analytic results for the integrals required.

The generalized moments in (2) and (3), for any m, are given by

$$\begin{aligned}
M &= -\mathrm{i}\,Q(t)\left(b(t) + 4\sqrt{m}\,\frac{k_t}{k_a}\,c(t)\,w(t)\right),\\
I_1 &= Q(t)\left(2\sqrt{m}\,\frac{k_t}{k_a}\,w(t) + x_0(t)\right),\\
I_2 &= 4\,\frac{k_b}{k_a}\,Q(t)\,w^2(t), \qquad (15)\\
I_3 &= \frac{16\,\mathrm{i}}{3\,k_a}\,w(t)\,Q(t)\left(3\,k_b c(t)\,w(t) - \sqrt{m}\,k_c\,b(t)\right),
\end{aligned}$$

where the constants k_i are given by the following expressions:

$$
\begin{aligned}
k_a &= \Gamma\left(\frac{1}{4}\right) H\left(\frac{1}{2},\frac{3}{4};m\right) + 8m\Gamma\left(\frac{3}{4}\right) H\left(\frac{5}{4},\frac{3}{2};m\right),\\
k_t &= \Gamma\left(-\frac{1}{4}\right) H\left(\frac{1}{2},\frac{5}{4};m\right) + 2m\Gamma\left(-\frac{3}{4}\right) H\left(\frac{3}{2},\frac{7}{4};m\right),\\
k_b &= \Gamma\left(\frac{3}{4}\right) H\left(\frac{1}{4},\frac{1}{2};m\right) + 8m\Gamma\left(\frac{5}{4}\right) H\left(\frac{3}{4},\frac{3}{2};m\right),\\
k_c &= 3\Gamma\left(\frac{3}{4}\right) H\left(\frac{1}{2},\frac{5}{4};m\right) + 8m\Gamma\left(\frac{5}{4}\right) H\left(\frac{3}{2},\frac{7}{4};m\right). \qquad (16)
\end{aligned}
$$

In these terms, we have used the function $H(r,s;m)$ to represent the generalized hypergeometric function ${}_0F_2\left(\{\};r,s;m^2\right)$.

For $m \to 0$, we thus get the expected results for a symmetric function. Now, we are in a position to take the derivatives of (15) with respect to t and equate them with the right hand sides of (4). After rearrangement, we obtain five coupled ODEs for the t-dependent parameters. By solving the ODEs, we obtain equations for evolution of soliton parameters. In particular, we find that solitons can have a non-zero velocity in a certain range of the original equation parameters. All soliton parameters in this region are oscillating. This solution is a limit cycle in the five-dimensional phase space. Two projections of this limit cycle into a two-dimensional plane of parameters are shown in Fig. 11. For lower values of ε, the parametric plot tends to a round shape, and hence the velocity of the center of mass and the energy Q are approximately sinusoidal functions of t. Indeed, with $\varepsilon = 1.29$, the velocity appears to be almost sinusoidal. For larger values of ε, the parametric plot becomes more elongated. This kind of irregularity is more evident as ε reaches the upper boundary of the creeping range. The closed curve parametric plots become larger in area since both x_0' and Q have a larger range of oscillations as ε increases.

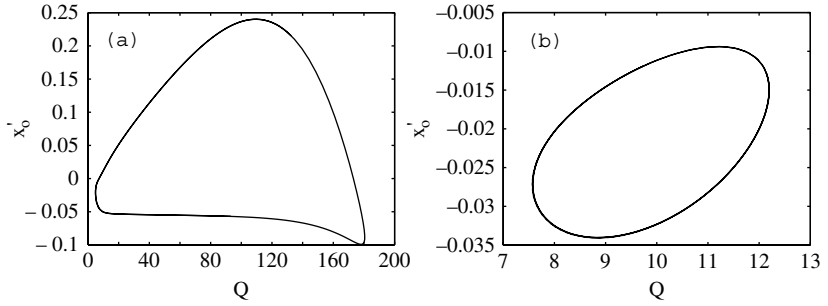

Fig. 11 Parametric plots of the soliton velocity x_0' vs energy Q for (**a**) $\varepsilon = 1.45$ and (**b**) $\varepsilon = 1.29$. Other parameters for this calculation are chosen as $D = 1$, $\delta = -0.1$, $\beta = 0.101$, $\mu = -0.3$, $\nu = -0.101$, while $m = 0.0025$. This value of m gives reasonably good agreement with the numerical solutions of the CGLE

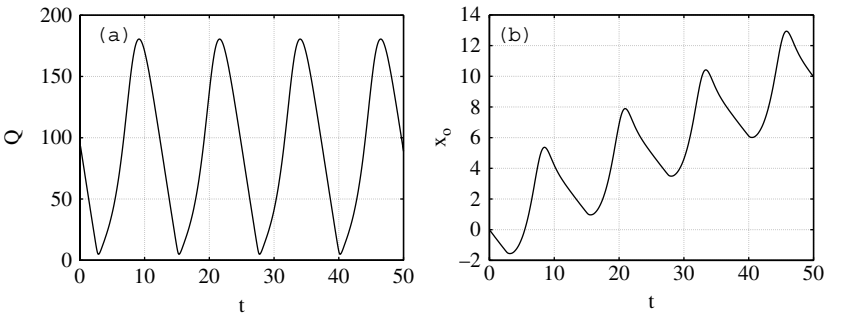

Fig. 12 (**a**) Soliton energy Q and (**b**) center of mass x_0 along the propagation t for a creeping soliton in the reduced model with $\varepsilon = 1.45$. Other parameters for this calculation are chosen as $D = 1$, $\delta = -0.1$, $\beta = 0.101$, $\mu = -0.3$, $\nu = -0.101$, while $m = 0.0025$

Periodic evolution of the energy Q and zig-zag type motion of the center of mass of the soliton x_0 along t are shown in Fig. 12. Qualitatively, these curves are similar to those shown in Fig. 10. Clearly, we cannot expect a better fit because of the dramatic reduction of the number of degrees of freedom when using the trial function. However, the possibility of modeling of the creeping solitons using a simple trial function is remarkable in itself.

The results for the region of existence of creeping solitons in a low-dimensional approximation are shown in Fig. 13. Similar to the numerical results, the creeping solitons occur in a central diagonal strip in Fig. 13. For lower values of ε, the limit cycle contracts to a fixed point with all parameters including the velocity being constant. This transition is a Hopf bifurcation. Thus, below the diagonal strip, we have solitons with constant shape and constant velocity the same way as in numerical simulations.

As ε increases, the period of all five parameters increases. At the upper limit of existence of creeping solitons, the soliton becomes wider while retaining a constant

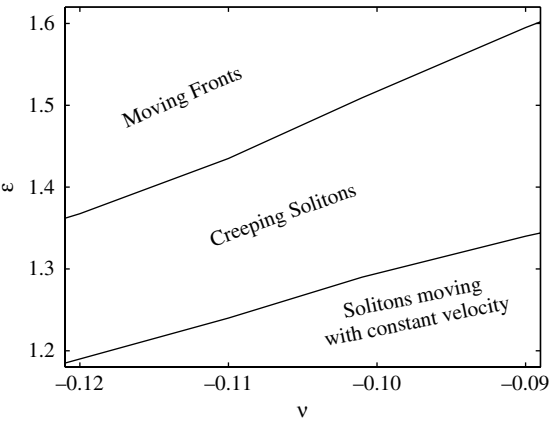

Fig. 13 Region of existence of creeping solitons in $(\varepsilon - \nu)$ plane. Here, $D = 1$, $\delta = -0.1$, $\beta = 0.101$, $\mu = -0.3$, while we set $m = 0.0025$. For $\nu = -0.101$, the transition from fixed point to creeping soliton occurs at $\varepsilon \approx 1.29$, while the bifurcation from creeping to moving fronts occurs at $\varepsilon = \varepsilon_0 \approx 1.5092$

amplitude, so the energy Q becomes approximately proportional to the width. At the top of the "creeping" range, the period becomes infinite, and there is a bifurcation to solitons with constantly increasing width. This behavior corresponds to the splitting of a soliton into a pair of fronts moving away from each other in numerical simulations. However, the velocity of the center of mass for this soliton is not zero, as was the case in the numerical simulations. Thus, in our reduced model we have only a single boundary separating creeping solitons from moving fronts (see Fig. 13). Again, this is hardly surprising if we take into account the drastic reduction in the number of degrees of freedom in our simplified model. Despite these discrepancies, the qualitative location of the region of existence of the creeping solitons and the boundary slopes are remarkably similar to those obtained in the numerical simulations.

6 Solitons and Antisolitons [28]

To conclude our chapter, we give one more example where soliton modeling using a simple trial function can be useful. In particular, this approach allows us to predict the existence of one more branch of stationary solitons that could be important for applications. Due to the many parameters which appear in the CGLE, finding all the branches using numerical simulations of it is indeed a difficult task.

To find the stationary solitons, we shall use again the trial function (9) and the corresponding dynamical system (11). Stationary solutions of (11) are given by the soliton parameters which are t independent, i.e., $Q(t) = Q_0$, $w(t) = w_0$ and $c(t) = c_0$. The latter case corresponds to a fixed point (FP) of the dynamical system (11). Fixed points of this three-variable dynamical system, together with the trial function (9), approximate the stationary solitons of the CGLE. Standard linearization techniques can be used to find the stability of these FPs. Unstable FPs usually correspond to unstable solitons. Stable FPs may correspond to stable solitons, but this has to be confirmed by direct numerical simulations of the CGLE. This is related to the fact that an infinite-dimensional dynamical system has more degrees of freedom to develop a soliton instability.

Solving the dynamical system (11) for various ε, μ and ν, regions of stable and unstable fixed points can be constructed in the space of these three parameters of the CGLE. Two plots representing the regions of stable and unstable FPs for fixed values of D, δ and β are shown in Fig. 14a and b. Each plot is a two-dimensional slice of the six-dimensional space of the equation parameters. Each of these plots clearly shows the existence of two separate regions of stable fixed points. A point from one region cannot be transformed into a point from the other region with a continuous change of parameters. Thus, it appears that these two regions correspond to two different types of solitons of the CGLE. One of the branches has high energy, Q_0, while the other one has low energy. Within the low-dimensional approximation (11), these FPs are stable in both regions. However, the results for the stability of exact CGLE solitons may differ, as we explained above.

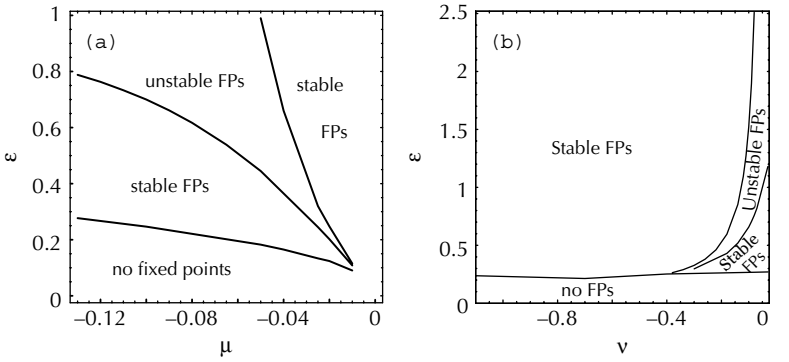

Fig. 14 Soliton bifurcation diagram (**a**) on the $\varepsilon - \mu$ plane and (**b**) on the $\varepsilon - \nu$ plane. There are two regions of stable fixed points that correspond to two quite different branches of solitons. In (**a**), $\delta = -0.1$, $\nu = -0.08$ and $\beta = 0.08$. In (**b**), $\mu - 0.1$, $\delta = -0.1$ and $\beta = 0.125$

Direct simulations of the CGLE (1) confirm the predictions made using the low-dimensional approximation. Figure 15a, numerically obtained, shows regions in the (μ, ε) plane where stationary localized solutions can be found. As predicted by the simple model, there are two separate regions in the parameter space where dissipative solitons exist. The gray regions correspond to stable stationary solitons while the hatched region corresponds to exploding solitons [31, 44, 46]. A comparison between Fig. 14a and Fig. 15a shows that there is not only a qualitative agreement between them, but that they also coincide reasonably well quantitatively. Our simple model, of course, cannot describe the explosive instability that is related to many

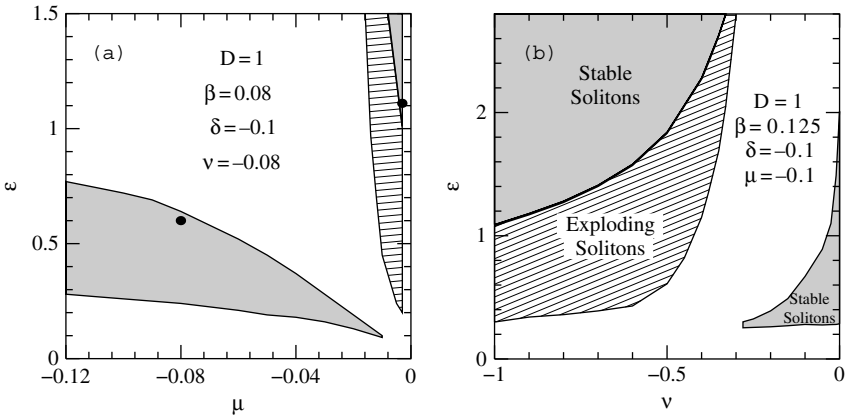

Fig. 15 Regions of existence of the two types of solitons (gray) in (**a**) (ε, μ) and (**b**) (ε, ν) plane. In each case, the two separate regions are quite distinct. Parameters are shown in the plot. The hatched region corresponds to exploding solitons

degrees of freedom of the CGLE solitons [46]. Thus, explosive solitons in a simple model will be in the area of stable fixed points. If we take this into account, the correspondence between the exact numerical results and the predictions of the low-dimensional approximation is remarkably close.

Figure 15b compiles the results of numerical simulations of the CGLE for the plane of parameters (ν, ε). Again, gray regions are for stable solitons while the hatched region is for exploding solitons. Comparing these results with those in Fig. 14b again shows a good qualitative agreement.

The results for the exact field amplitude and phase profiles of the solutions for each region of existence of stable solitons are presented in Fig. 16. The solid lines represent the field amplitude of the solitons, while the dashed lines are their phase profiles. The upper curves (a) in Fig. 16 correspond to the upper-right thick black point in Fig. 15a and vice versa: the lower curves (b) in Fig. 16 correspond to the lower-left thick black point. There are some obvious differences in the energies, widths and amplitudes of the two solitons. However, the most visible qualitative difference is in the soliton chirp. The phase profiles clearly show that the chirps in the two cases are of opposite signs. Due to this difference, the energy flows from the inside to the outside of the soliton in the first case while it flows inwards in the second case.

The results obtained from the finite dimensional model (11) show that, for Fig. 14a, the upper right corner region has $c_0 > 0$ and it is large in magnitude, i.e., there is a strong chirp across the soliton. On the other hand, the stable FP on the lower left region has $c_0 < 0$ and it is small in magnitude, so the soliton is weakly chirped. As regards Fig. 14b, we have $c_0 < 0$ in the lower right hand corner region (low energy Q_0), while we find $c_0 > 0$ in the upper left corner region (high energy Q_0). The same patterns for the chirp signs are obtained in the two distinct regions in Fig. 15a and b when directly solving the CGLE.

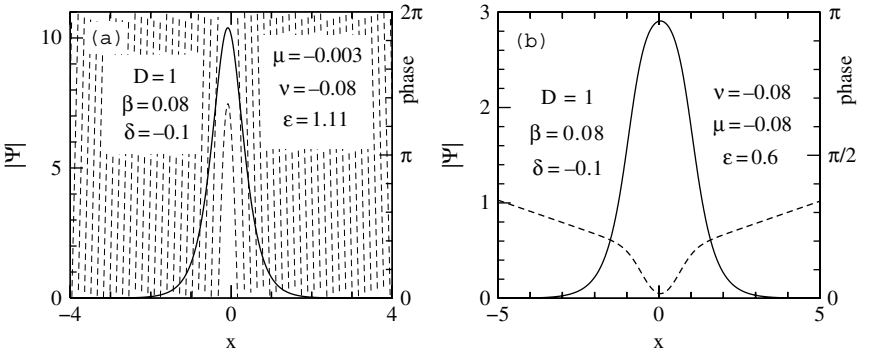

Fig. 16 Exact soliton profiles (*solid lines*) of two examples in the (**a**) upper and (**b**) lower regions in Fig. 15b. They are marked by thick black dots in Fig. 15b. *Dashed lines* show their corresponding phase profiles

The finite-dimensional model can be used to directly relate the chirp to the energy generation $P(x)$ and flux $j(x)$ (see Sect. 6 of [25]). Using the trial function (9) for arbitrary m, with $A = \sqrt{\frac{Q_0}{w_0}}$, for stationary solutions we find

$$j(x) = \frac{\mathrm{i}}{2}(\psi\,\psi_x^* - \psi_x\,\psi^*) = c_0\,GX\,\exp\left[-2X^2\left(1+\frac{X^2}{4m}\right)\right], \tag{17}$$

and

$$P(x) = \frac{\mathrm{d}j}{\mathrm{d}x} = c_0\,\frac{G}{w_0}\left(1-4X^2-\frac{2}{m}X^4\right)\exp\left[-2X^2\left(1+\frac{X^2}{4m}\right)\right], \tag{18}$$

where $G = 2a^2(m)\,Q_0$ and the normalized transverse variable $X = x/w_0$. We have the condition that the total energy generation is zero:

$$\int_{-\infty}^{\infty} P(x)\,\mathrm{d}x = 0. \tag{19}$$

This condition has to be satisfied for stationary solutions and is clearly valid for these trial functions.

The curves for P divided by c_0G/w_0 and j divided by c_0G are shown in Fig. 17. It is clear that both the flux, j, and energy generation, P, change signs with c_0, since they are directly proportional to c_0 ($M > 0$, and $w_0 > 0$). Thus, the sign of the chirp has an important physical implication. If $c_0 < 0$, then $P > 0$ in the wings and $P < 0$ around the pulse center. This means that energy is generated in the wings and flows toward the middle, where it is dissipated. Conversely, if $c_0 > 0$, then $P < 0$ in the wings and $P > 0$ around the pulse center, so energy is generated in the middle and flows toward the wings, where it is lost. This process, involving an internal flux of energy, produces the dynamic equilibrium which we call a dissipative soliton.

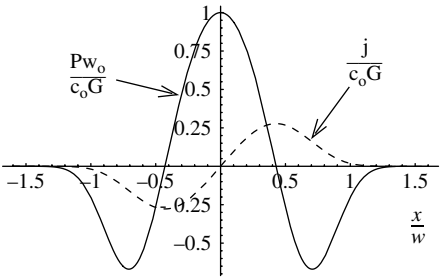

Fig. 17 Density of energy generation P across the soliton divided by c_0G/w_0 (*solid line*) and energy flux j divided by c_0G (*dashed line*) for low-dimensional model with $m = 1/4$. If $c_0 > 0$, then the curve shapes for P and j are as shown here so that energy is generated in the center. However, the curves for P and j are plainly inverted if $c_0 < 0$, and then the energy is dissipated in the center

The different signs of chirp appearing for each region (high Q and low Q) mean that the phase profile across the soliton is concave up in one case and concave down in the other. Hence, we can designate them "solitons" and "antisolitons" for convenience. The phase profile for the CGLE solitons is not exactly parabolic, of course, but it is clear from Fig. 16a and b that the effective chirp coefficients are opposite in sign and that the chirp magnitude in Fig. 16a is much greater than that in Fig. 16b.

For comparison, we plot the distribution of energy generated and dissipated inside of the two types of the CGLE solitons in Fig. 18a and b. We can see clearly that in the first case (a), the energy generation is positive in the middle of the soliton and negative in the wings, while in the second case (b), the energy is generated in the tails of the soliton and dissipated in the middle. Thus, there is a fundamental qualitative difference between the two types of solitons. One type cannot be transformed into the other with a continuous change of parameters. To be specific, we call the solitons with lower energy and $c_0 < 0$ (ordinary) dissipative solitons and the localized solutions of the upper branch (with $c_0 > 0$) "dissipative antisolitons". The fact that antisolitons have much higher energy than solitons may have important consequence for the development of high-power pulse-generating passively mode-locked lasers. It is very likely that antisolitons have been already observed experimentally in the recent paper [47].

Above, we have presented three examples of approximate analysis of dissipative solitons and bifurcations between them. These give some flavor of what can be done analytically in the study of soliton transformations of the CGLE. In these examples, we were able to describe bifurcations between stationary and pulsating solitons as well as bifurcations between pulsating and creeping solitons. The approach also allowed us to predict the existence of a new branch of stationary solitons, and this was then confirmed by direct numerical simulations. Taking into account the fact that several system parameters control bifurcations of CGLE solitons, it is hard to imagine that any other technique would give similar results.

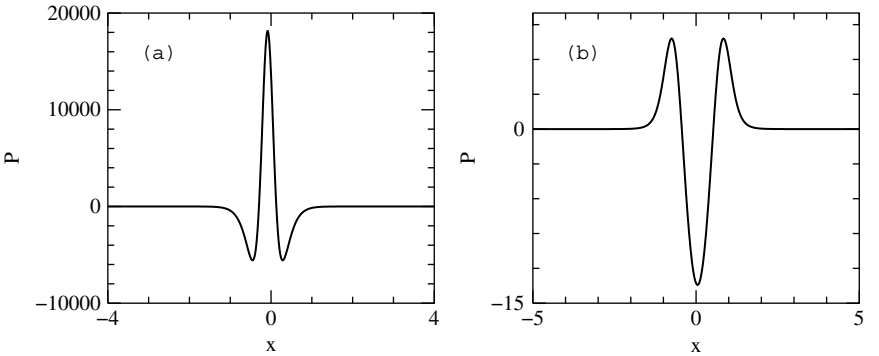

Fig. 18 Energy generation, P, inside the two types of solitons shown in Fig. 16. In (**a**), the energy is generated in the middle of the soliton and is dissipated in the tails, while in (**b**), it is generated in the tails and dissipated in the center

7 Conclusions

The notion of the dissipative soliton has emerged from a three-part foundation. To be specific, these parts are classical soliton theory, nonlinear dynamics (with its theory of bifurcations) and Prigogine's concept of self-organization. These underlying ideas set us up for a comprehensive understanding of the new notion and allow us to explain the basic properties of solitons in dissipative systems. Complications which arise from the fact the dynamical systems usually have an infinite number of degrees of freedom can be overcome by using reductions to low-dimensional systems. However, these reductions always need to be done carefully by comparing the conclusions with the results of particular numerical simulations of the original equation.

Acknowledgements The authors acknowledge support from the Australian Research Council (Discovery Project DP0663216).

References

1. N. Akhmediev and A. Ankiewicz, Solitons around us: Integrable, Hamiltonian and dissipative systems, in *Optical Solitons: Theoretical and Experimental Challenges*, Edited by K. Porsezian and V.C. Kurakose, (Springer, Berlin-Heidelberg, 2003), pp. 105–126.
2. N. Akhmediev and A. Ankiewicz, Solitons of the complex Ginzburg–Landau equation, in *Spatial Solitons* 1, Edited by S. Trillo and W.E. Toruellas, (Springer, Berlin-Heidelberg, 2001), pp. 311–342.
3. N. Akhmediev, General theory of solitons, in *Soliton-Driven Photonics*, edited by A.D. Boardman and A.P. Sukhorukov, (Kluver Academic Publishers, Netherlands, 2001), pp. 371–395.
4. N.J. Zabusky and M.D. Kruskal, Interaction of 'solitons' in a collisionless plasma and the recurrence of initial states, Phys. Rev. Lett. **15**, 240–243 (1965).
5. J.S. Russell, Report of the fourteenth meeting of the British Association for the Advancement of Science, York, 1844 (London 1845), pp. 311–390, Plates XLVII-LVII.
6. C.S. Gardner, J.M. Greene, M.D. Kruskal, and K.M. Miura, Method for solving the Korteweg–de Vries equation, Phys. Rev. Lett. **19**, 1095–1097 (1967).
7. V.E. Zakharov and A.B. Shabat, Exact theory of two dimensional self focusing and one dimensional self modulation of nonlinear waves in nonlinear media, *Sov. Phys. JETP*, **34**, 62–69 (1971)]. Original (in Russian): Zh. Eksp. Teor. Fiz. **61**, 118.
8. M.J. Ablowitz and P.A. Clarkson, *Solitons, Nonlinear Evolution Equations and Inverse Scattering*, London Mathematical Society Lecture Notes Series **149**, (Cambridge University Press, Cambridge, (1991).
9. G.P. Agrawal, *Nonlinear Fiber Optics*, 2nd edn, (Academic Press Inc., San Diego, CA, 1995).
10. E. Picholle, C. Montes, C. Leycuras, O. Legrand, and J. Botineau, Observation of dissipative superluminous solitons in a Brillouin fiber ring laser, Phys. Rev. Lett. **66**, 1454 (1991).
11. C.I. Christov and M.G. Velarde, Dissipative solitons, Physica D, **86**, 323–347 (1995).
12. Akhmediev, N., Ankiewicz, A. (eds.): *Dissipative Solitons*. Lect. Notes Phys. **V. 661**. Springer, Heidelberg (2005).
13. B.S. Kerner and V.V. Osipov, *Autosolitons: A New Approach to Problems of Self-Organization and Turbulence, Fundamental Theories of Physics*, **61**, (Kluwer Academic Publishers, Dordrecht, 1996).

14. H.-G. Purwins, H.U. Bödeker and A.W. Liehr, Dissipative Solitons in Reaction-Diffusion Systems, Chapter 10 in the book [12].
15. H. Haken, *Synergetics*, (Springer-Verlag, Berlin, 1983).
16. N. Bekki and K. Nozaki, Formations of spatial patterns and holes in the generalized Ginzburg–Landau equation, Phys. Lett. A, **110**, 133–135 (1985).
17. W. Van Saarloos and P.C. Hohenberg, Fronts, pulses, sources and sinks in generalized complex Ginzburg–Landau equations, Physica D **56**, 303–367 (1992).
18. N. Akhmediev and V. Afanasjev, Novel arbitrary-amplitude soliton solutions of the cubic–quintic complex Ginzburg–Landau equation, Phys. Rev. Lett. **75**, 2320–2323 (1995).
19. V.B. Taranenko, K. Staliunas, and C.O. Weiss, Spatial soliton laser: Localized structures in a laser with a saturable absorber in a self-imaging resonator, Phys. Rev. A **56**, 1582–1591 (1997).
20. W.J. Firth and A.J. Scroggie, Optical bullet holes: Robust controllable localized states of a nonlinear cavity, Phys. Rev. Lett. **76**, 1623–1626 (1996).
21. N.A. Kaliteevstii, N.N. Rozanov, and S. Fedorov, V. Formation of laser bullets, Opt. Spectrosc. **85**, 533–534 (1998).
22. D. Mihalache, D. Mazilu, F. Lederer, H. Leblond, and B.A. Malomed, Stability of dissipative optical solitons in the three–dimensional cubic–quintic Ginzburg-Landau equation, Phys. Rev. A **75**, 033811 (2007).
23. J.M. Soto-Crespo, N. Akhmediev, and Ph. Grelu, Optical bullets and double bullet complexes in dissipative systems, Phys. Rev. E **74**, 046612 (2006).
24. D. Michaelis, U. Peschel, and F. Lederer, Oscillating dark cavity solitons, Opt. Lett. **23**, 1814–1816 (1998).
25. N. Akhmediev and A. Ankiewicz, Dissipative Solitons in the Complex Ginzburg–Landau and Swift-Hohenberg Equations, Chapter 1 in [12].
26. I.S. Aranson and L. Kramer, The world of the complex Ginzburg–Landau equation, Rev. Mod. Phys. **74**, 100 (2002).
27. J.M. Soto-Crespo, N. Akhmediev, and V.V. Afanasjev, Stability of the pulselike solutions of the quintic complex Ginzburg–Landau equation, JOSA B **13**, No 7, 1439–1449, (1996).
28. A. Ankiewicz, N. Devine, N. Akhmediev, and J.M. Soto-Crespo, Dissipative solitons and antisolitons, Phys. Lett. A **368**, September (2007).
29. N. Akhmediev, J.M. Soto-Crespo, and Ph. Grelu, Vibrating and shaking soliton pairs in dissipative systems, Phys. Lett. A **364**, 413–416 (2007).
30. N. Akhmediev and A. Ankiewicz, *Solitons, Nonlinear Pulses and beams*, (Chapman and Hall, London, 1997).
31. N. Akhmediev, J.M. Soto-Crespo, and G. Town, Pulsating solitons, chaotic solitons, period doubling, and pulse coexistence in mode-locked lasers: CGLE approach, Phys. Rev. E **63**, 056602 (2001).
32. W. Chang, A. Ankiewicz, N. Akhmediev, and J.M. Soto-Crespo, Creeping solitons in dissipative systems and their bifurctaions, Phys. Rev. E **76**, 016607 (2007).
33. A.I. Maimistov, Evolution of solitary waves which are approximately solitons of a nonlinear Schrödinger equation, J. Exp. Theor. Phys. **77**, 727 (1993) [Zh. Eksp. Teor. Fiz. **104**, 3620 (1993), in Russian].
34. E.N. Tsoy and C.M. de Sterke, Propagation of nonlinear pulses in chirped fiber gratings, Phys. Rev. E **62**, 2882 (2000).
35. F.Kh. Abdullaev, D.V. Navotny, and B.B. Baizakov, Optical pulse propagation in fibers with random dispersion, Physica D **192**, 83 (2004).
36. M.N. Zhuravlev and N.V. Ostrovskaya, Dynamics of NLS solitons described by the cubic–quintic Ginzburg–Landau equation, J. Exper. Theor. Phys. **99**, 427 (2004) [Zh. Eksp. Teor. Fiz. **126**, 483 (2004), in Russian].
37. E. Tsoy and N. Akhmediev, Bifurcations from stationary to pulsating solitons in the cubic–quintic complex Ginzburg–Landau equation, Phys. Lett. A **343**, 417–422 (2005).
38. E. Tsoy, A. Ankiewicz, and N. Akhmediev, Dynamical models for dissipative localized waves of the complex Ginzburg–Landau equation, Phys. Rev. E **73**, 036621 (2006).

39. N. Akhmediev, A. Ankiewicz and J.M. Soto-Crespo, Stable soliton pairs in optical transmission lines and fiber lasers, J. Opt. Soc. Am. B **15**, 515 (1998).
40. J.M. Soto-Crespo, M. Grapinet, Ph. Grelu, and N. Akhmediev, Bifurcations and multiple period soliton pulsations in a passively mode-locked fiber laser, Phys. Rev. E **70**, 066612 (2004).
41. J. Guckenheimer and P. Holmes, *Nonlinear Oscillations, Dynamical Systems and Bifurcations of Vector Fields*, (Springer-Verlag, New York, 1983).
42. J. Satsuma and N. Yajima, Initial value-problems of one-dimensional self-modulation of nonlinear waves in dispersive media, Progr. Theor. Phys. Suppl. **55**, 284 (1974).
43. W. Chang, A. Ankiewicz, N. Akhmediev, and J.M. Soto-Crespo, Creeping solitons of the complex Ginzburg–Landau equation with a low-dimensional dynamical system model, Phys. Lett. A**362**, 31–36 (2007).
44. J.M. Soto-Crespo, N. Akhmediev and A. Ankiewicz, Pulsating, creeping, and erupting solitons in dissipative systems, Phys. Rev. Lett. **85**, 2937–2940, (2000).
45. H.P. Tian, Z.H. Li, J.P. Tian, G.S. Zhou and J. Zi, Effect of nonlinear gradient terms on pulsating, erupting and creeping solitons, Appl. Phys. B **78**, 199–204 (2004).
46. N. Akhmediev and J.M. Soto–Crespo, Exploding solitons and Shil'nikov's theorem, Phys. Lett. A **317**, 287–292 (2003).
47. A. Fernandez, T. Fuji, A. Poppe, A. Frbach, F. Krausz, and A. Apolonski, Chirped-pulse oscillators: A route to high-power femtosecond pulses without external amplification, Opt. Lett. **29**, 1366–1368 (2004).